Electronic Supplementary Material (ESI) for Journal of Materials Chemistry C.

Diazaspirocycles: Novel Platforms for Efficient Phosphorescent Organic Light-Emitting Diodes

Xiang-Yang Liu,† Yi-Jie Zhang,† Xiyu Fei, Quan Ran, Man-Keung Fung,* and Jian Fan*

Jiangsu Key Laboratory for Carbon-Based Functional Materials & Devices, Institute of Functional Nano & Soft Materials (FUNSOM), Soochow University, Suzhou, Jiangsu 215123, China

† The two authors contribute equally to this paper.

*E-mail: mkfung@suda.edu.cn (Prof. M.-K. Fung); jianfan@suda.edu.cn (Prof. J. Fan).

General Information

All chemicals and reagents were used as received from commercial sources without further purification. THF was purified by PURE SOLV (Innovative Technology) purification system. ^{1}H NMR and ^{13}C NMR spectra were recorded in chloroform-*d* ($CDCl_3$) on a Bruker 400 and Agilent DD2-600 MHz NMR spectrometer at room temperature. Matrix-Assisted Laser Desorption/ Ionization Time of Flight Mass Spectrometry (MALDI-TOF-MS) was measured with a BRUKER ultrafleXtreme MALDI-TOF/TOF. UV-vis absorption spectra were recorded on Cary 60 spectrometer (Agilent Technologies). PL spectra and phosphorescent spectra were recorded on a Hitachi F-4600 fluorescence spectrophotometer. Differential scanning calorimetry (DSC) was performed on a TA DSC 2010 unit at a heating rate of 10 ^{o}C min^{-1} under nitrogen. The glass transition temperatures (T_g) were determined from the second heating scan. Thermogravimetric analysis (TGA) was performed on a TA SDT 2960 instrument at a heating rate of 10 ^{o}C min^{-1} under nitrogen. Temperature at 5% weight loss was used as the decomposition temperature (T_d). Cyclic voltammetry (CV) was carried out on a CHI600 voltammetric analyzer at room temperature with ferrocenium-ferrocene (Fc^+/Fc) as the internal standard. The oxidative scans were performed using 0.1 M n-Bu_4NPF_6 ($TBAPF_6$) in deaerated DMF as the supporting electrolyte. A conventional three-electrode configuration consisting of a Pt-wire counter electrode, an Ag/AgCl reference electrode, and a platinum working electrode was used. The cyclic voltammograms were measureed at a scan rate of 100 mV s^{-1}. DFT calculations were performed using B3LYP/6-31 G(d) basis set using Gaussian 09.

Device Fabrication and Characterization

The OLEDs were fabricated on the indium-tin oxide (ITO) coated transparent glass substrates, the ITO conductive layer having a thickness of ca. 100 nm and a sheet resistance of ca. 30 Ω per-square. The active area of each device is 0.09 cm^2. The ITO glasses were ultrasonically cleaned by ethanol, acetone and deionized water for 10 min subsequently, and then exposed to UV-ozone for 15 min. All of the organic materials and metal layers under a vacuum of ca. 10^{-6} Torr. The deposition rate was controlled at

2 Å s^{-1} for HAT-CN, 0.2-0.4 Å s^{-1} for Liq, 1-2 Å s^{-1} for other organic layers and 5-8 Å s^{-1} for Al anode. The EL spectra, CIE coordinates, *J*-V-*L* curves, CE, and PE of the devices were measured with a programmable spectra scan photometer (PHOTO RESEARCH, PR 655) and a constant current source meter (KEITHLEY 2400) at room temperature.

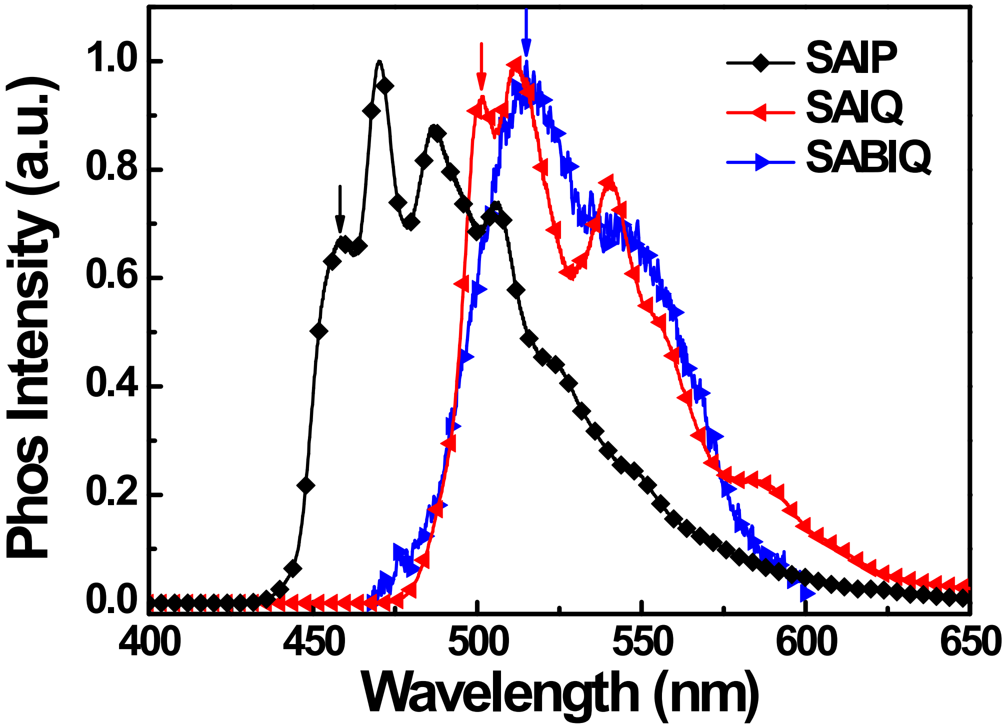

Figure S1. Low temperature Phos spectra of **SAIP**, **SAIQ**, and **SABIQ**.

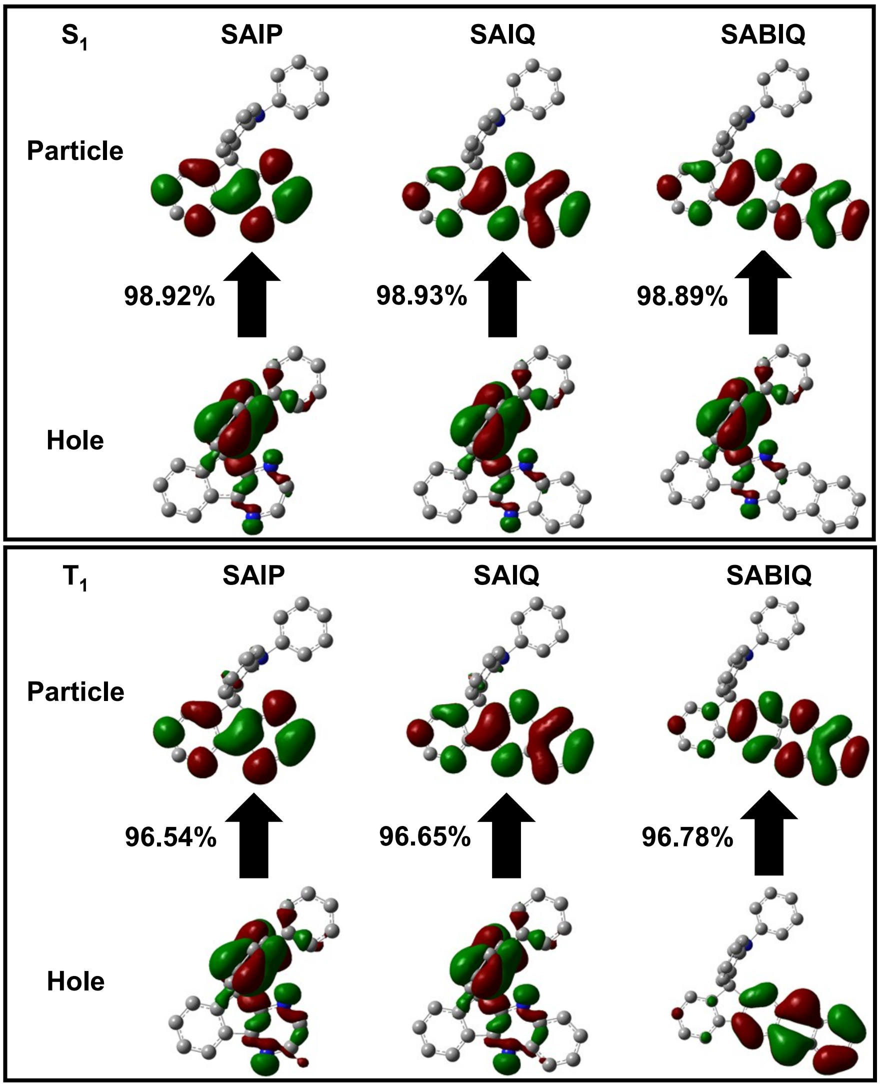

Figure S2. Natural transition orbitals (NTO) analyses of the singlet (S_1) and triplet (T_1) states for **SAIP**, **SAIQ**, and **SABIQ**.

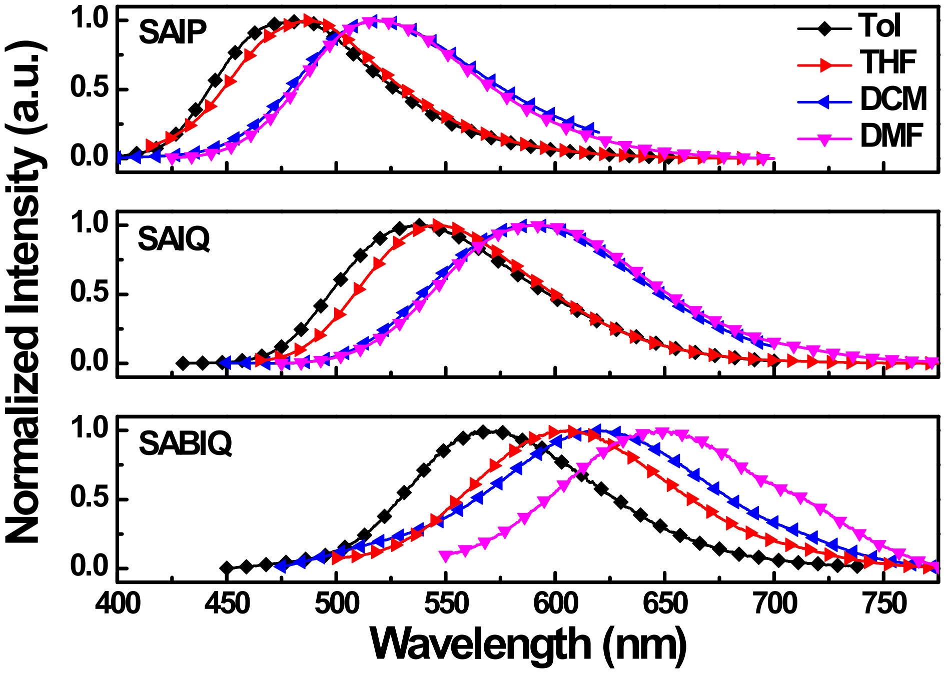

Figure S3. PL spectra of **SAIP**, **SAIQ**, and **SABIQ** in different solvent.

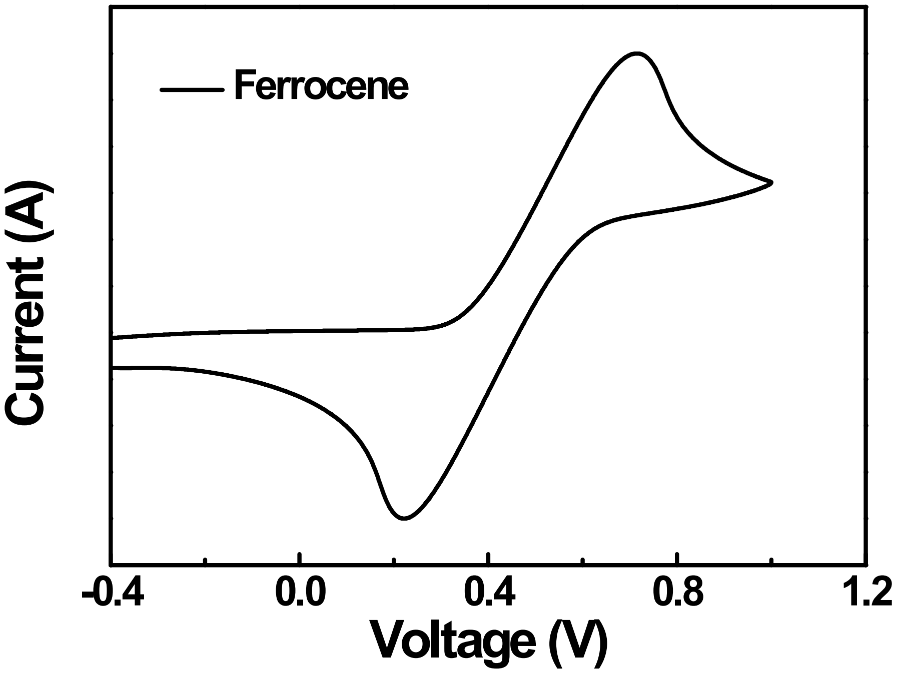

Figure S4. Cyclic voltammogram of ferrocene.

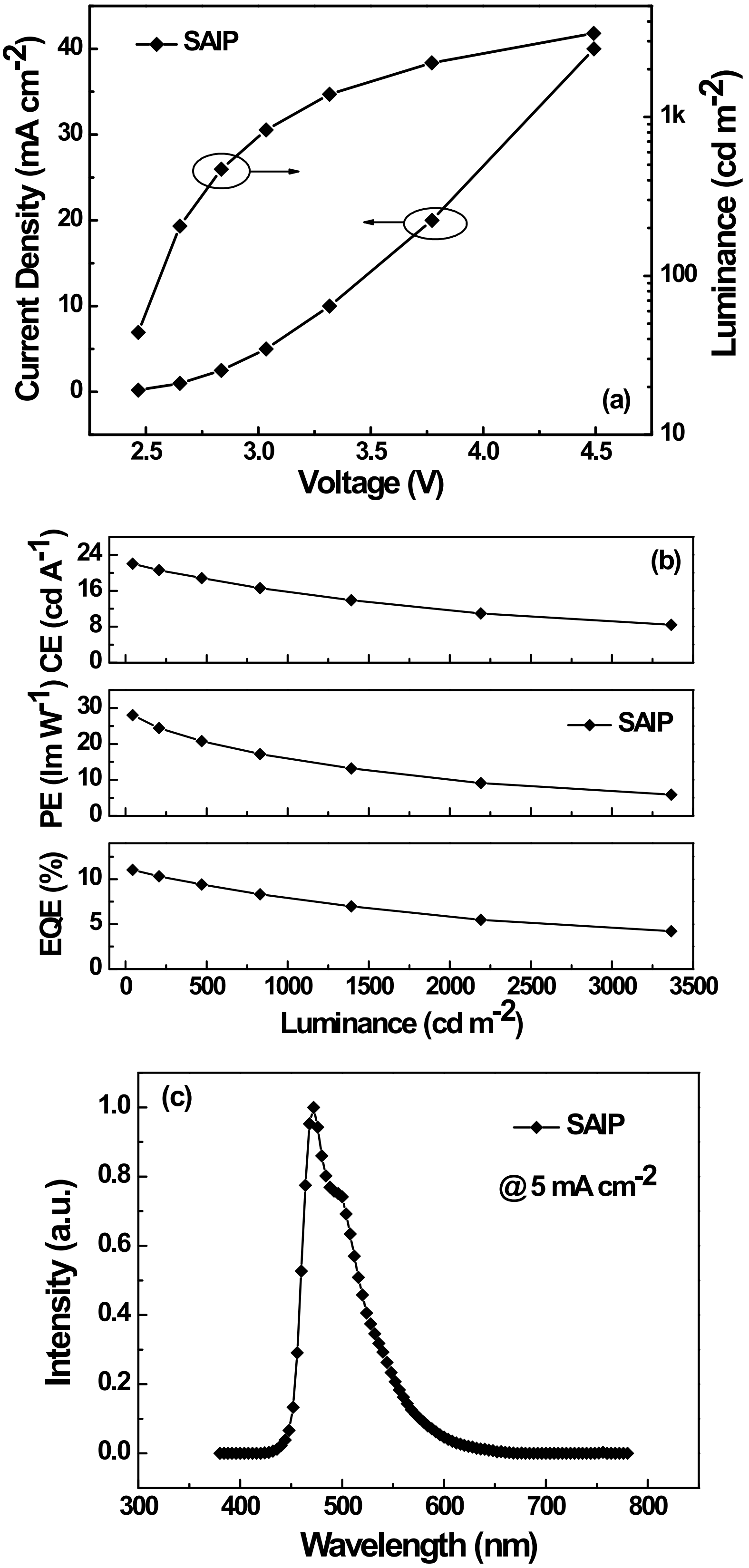

Figure S5. (a) *J*–V–*L* characteristics, (b) CE–, PE–, and EQE–*L* curves, and (c) EL spectrum of blue device.

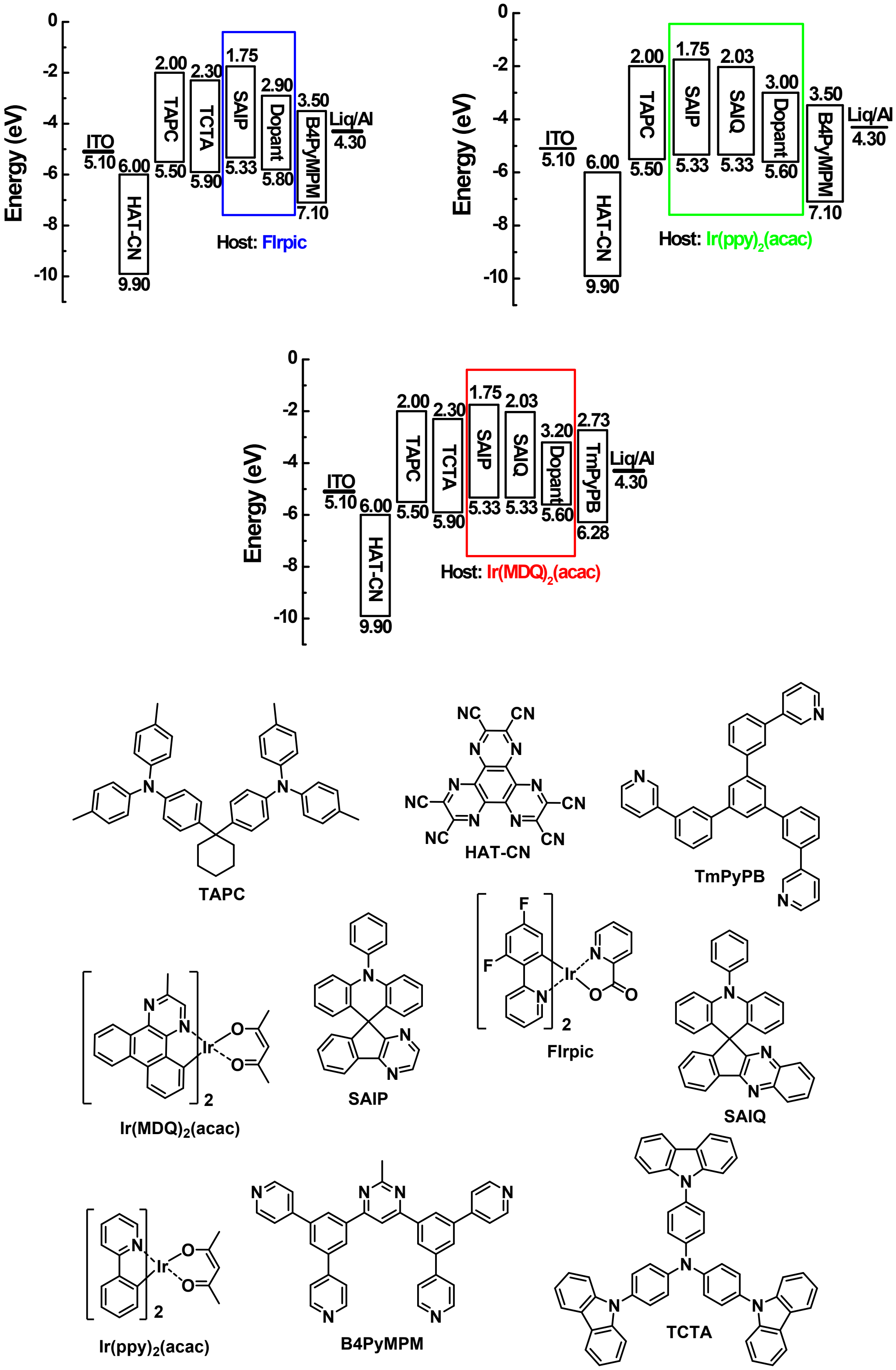

Figure S6. Blue, green, and red device structures and energy diagram and molecule structure of the materials.

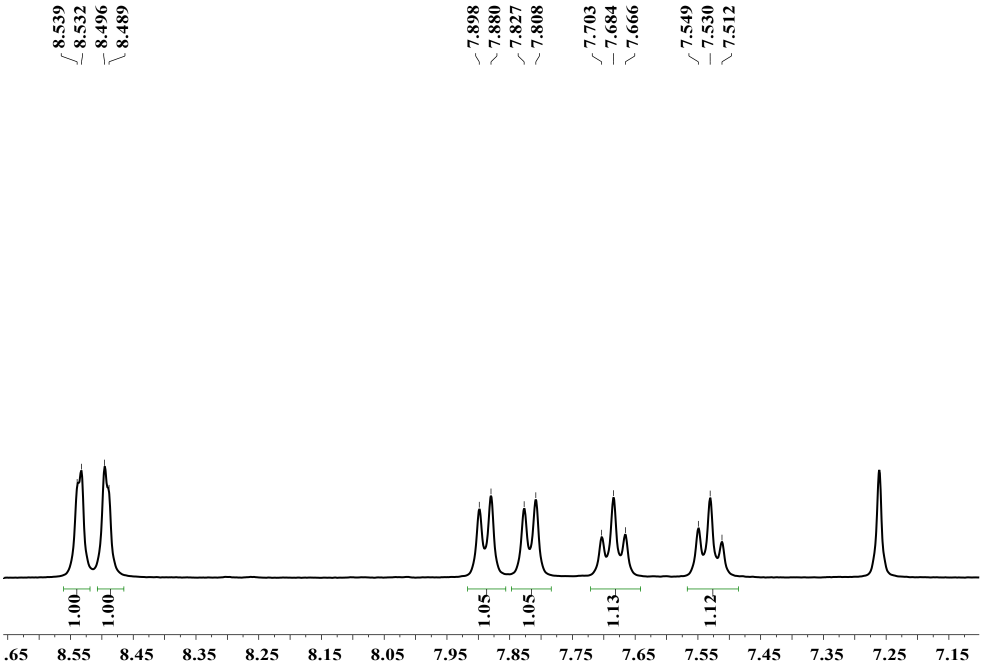

Figure S7. ^{1}H NMR of **1** (400 MHz, CDCl$_3$).

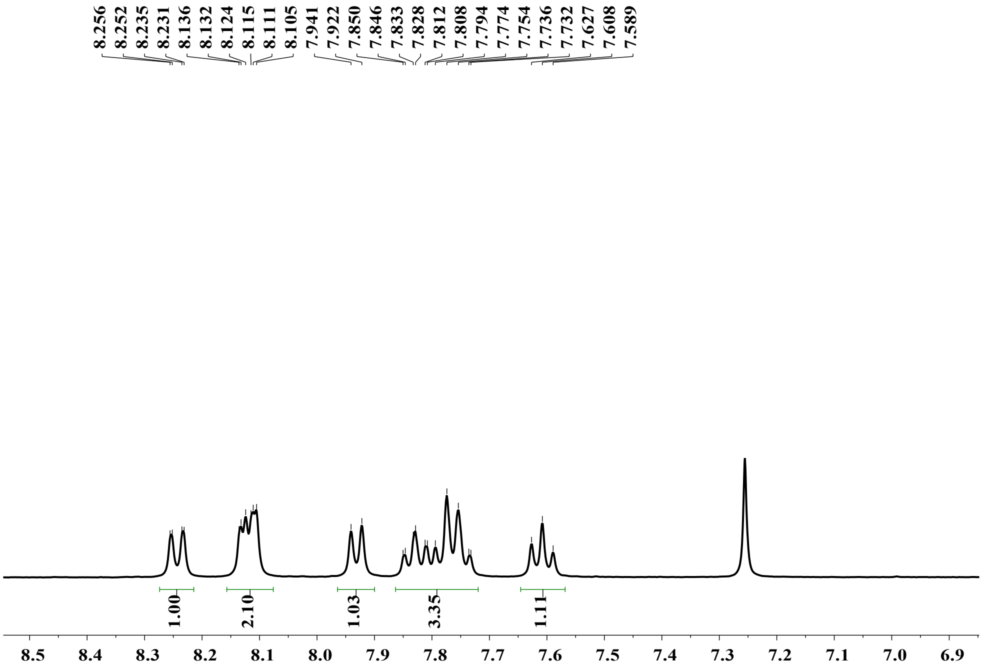

Figure S8. ^{1}H NMR of **2** (400 MHz, CDCl$_3$).

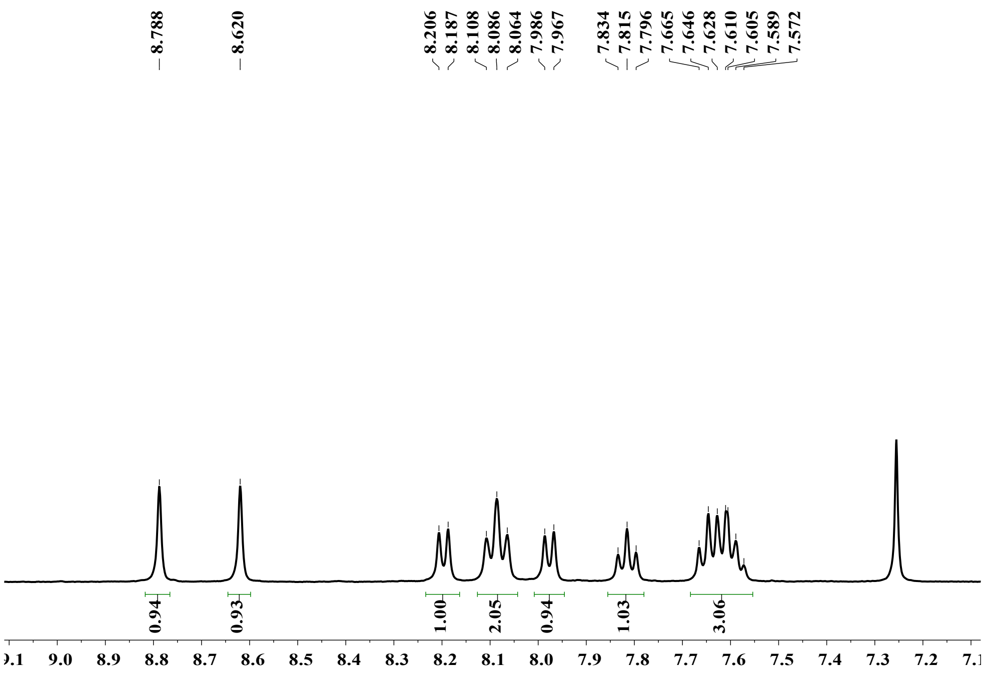

Figure S9. ^{1}H NMR of **3** (400 MHz, CDCl$_3$).

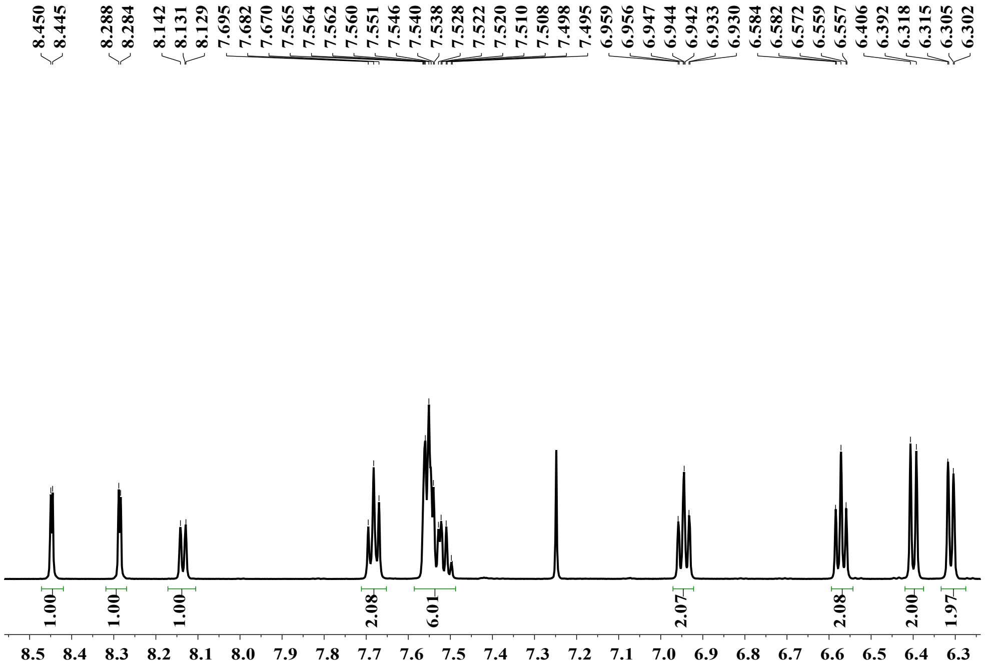

Figure S10. ^{1}H NMR of **SAIP** (600 MHz, CDCl$_3$).

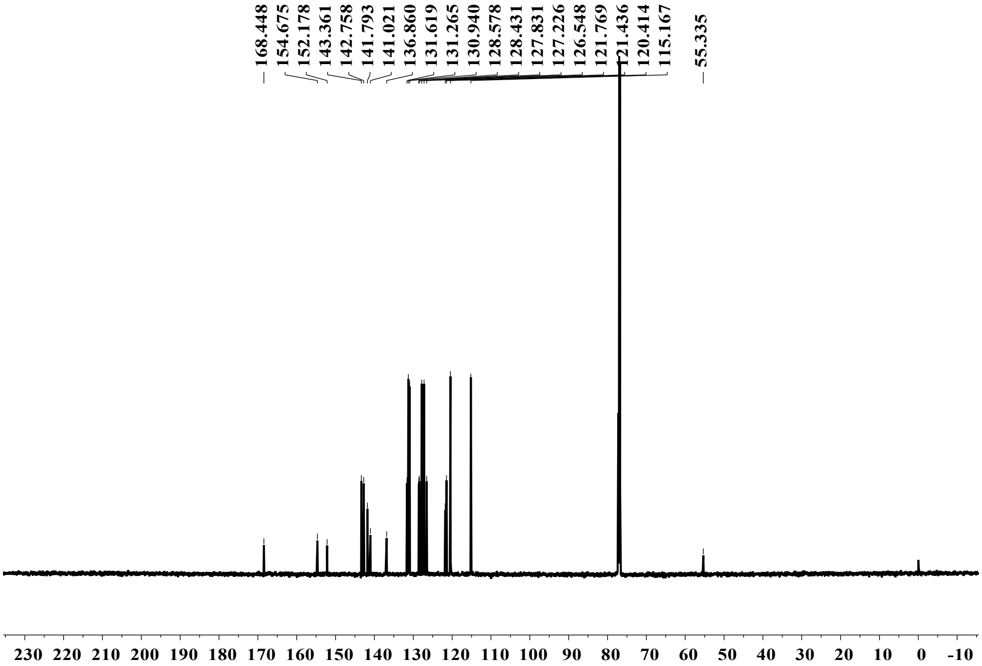

Figure S11. ^{13}C NMR of **SAIP** (151 MHz, CDCl$_3$).

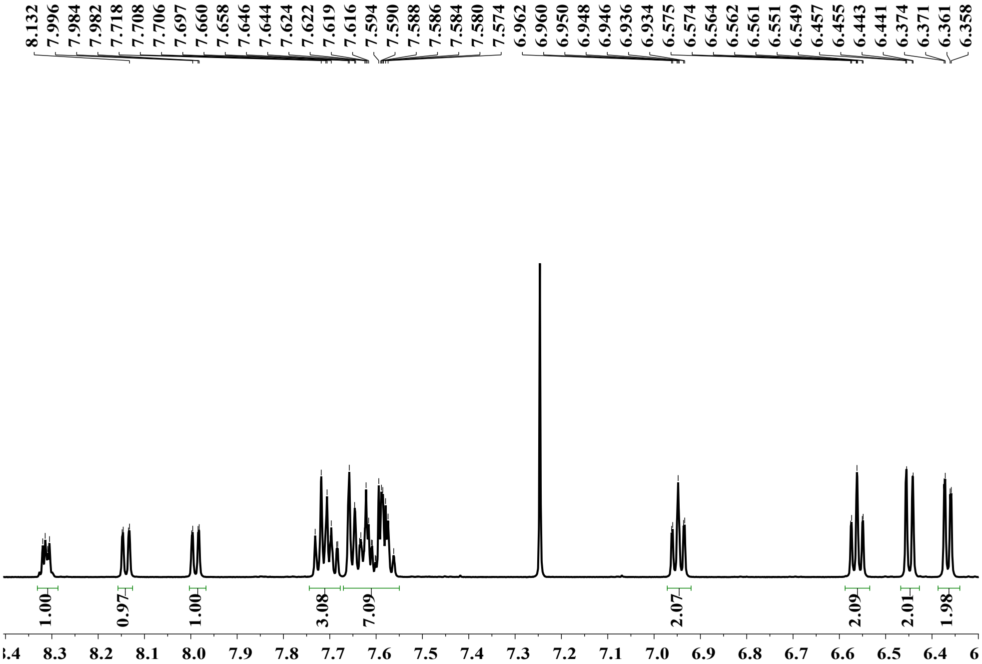

Figure S12. ^{1}H NMR of **SAIQ** (600 MHz, CDCl$_3$).

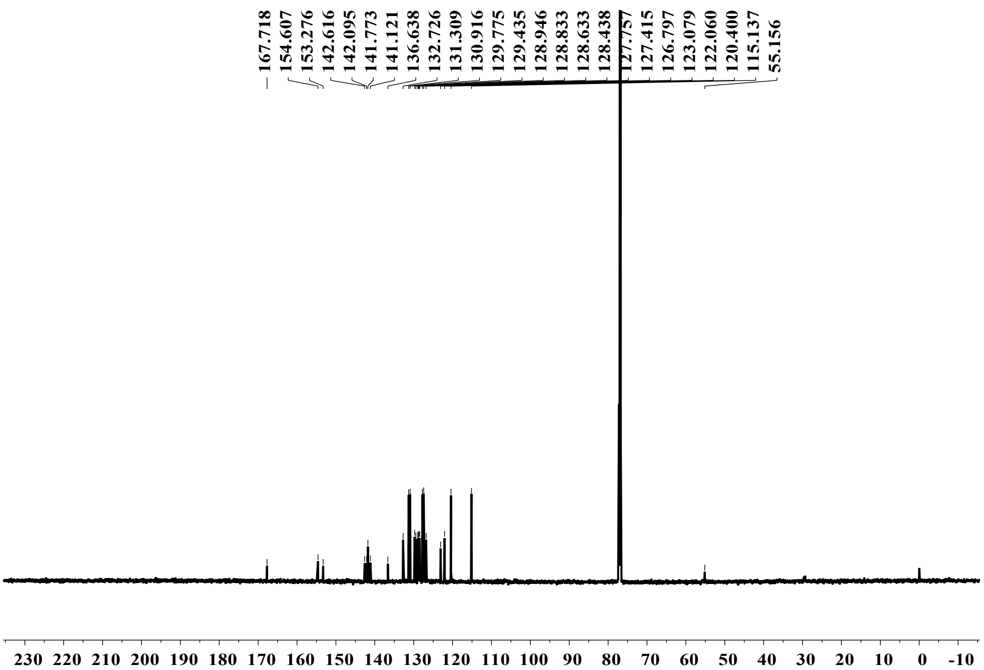

Figure S13. ^{13}C NMR of **SAIQ** (151 MHz, CDCl$_3$).

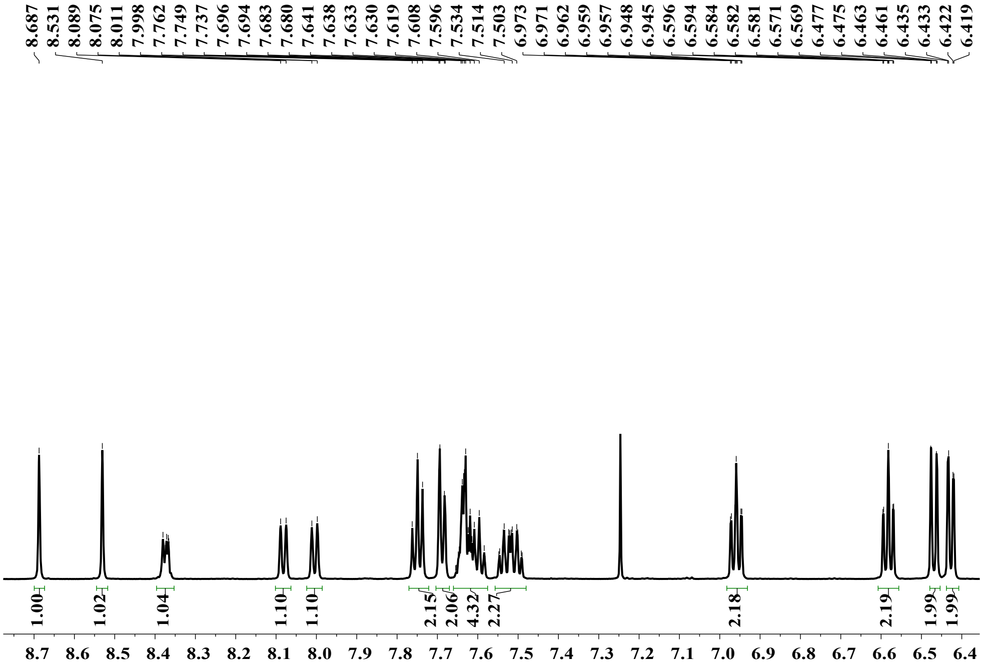

Figure S14. ^{1}H NMR of **SABIQ** (600 MHz, CDCl$_3$).

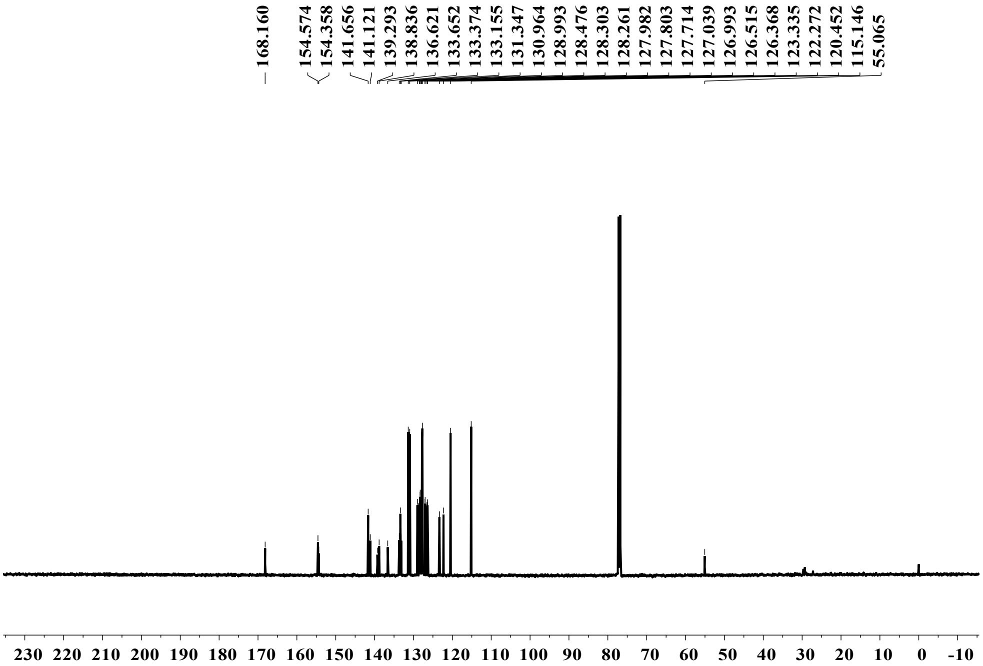

Figure S15. ^{13}C NMR of **SABIQ** (151 MHz, $CDCl_3$).

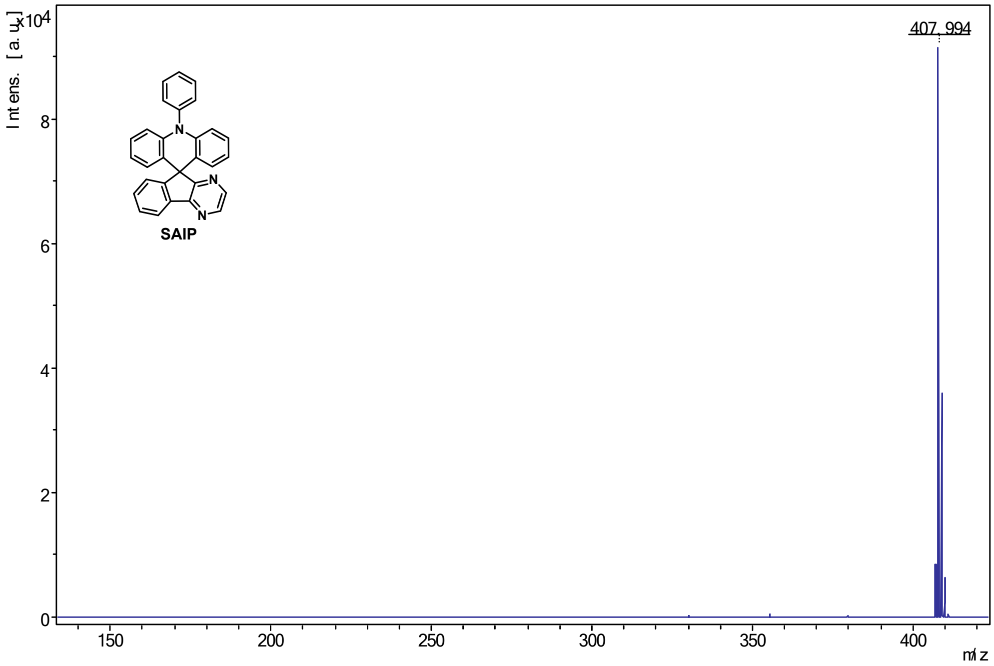

Figure S16. MALDI-TOF-MS spectrum of **SAIP**.

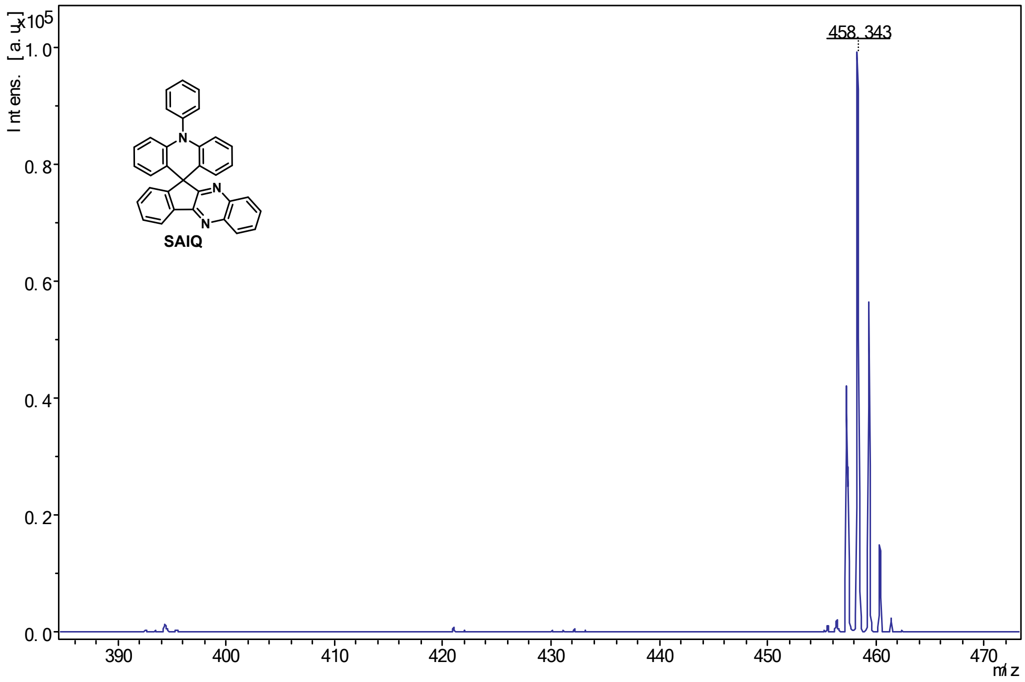

Figure S17. MALDI-TOF-MS spectrum of **SAIQ**.

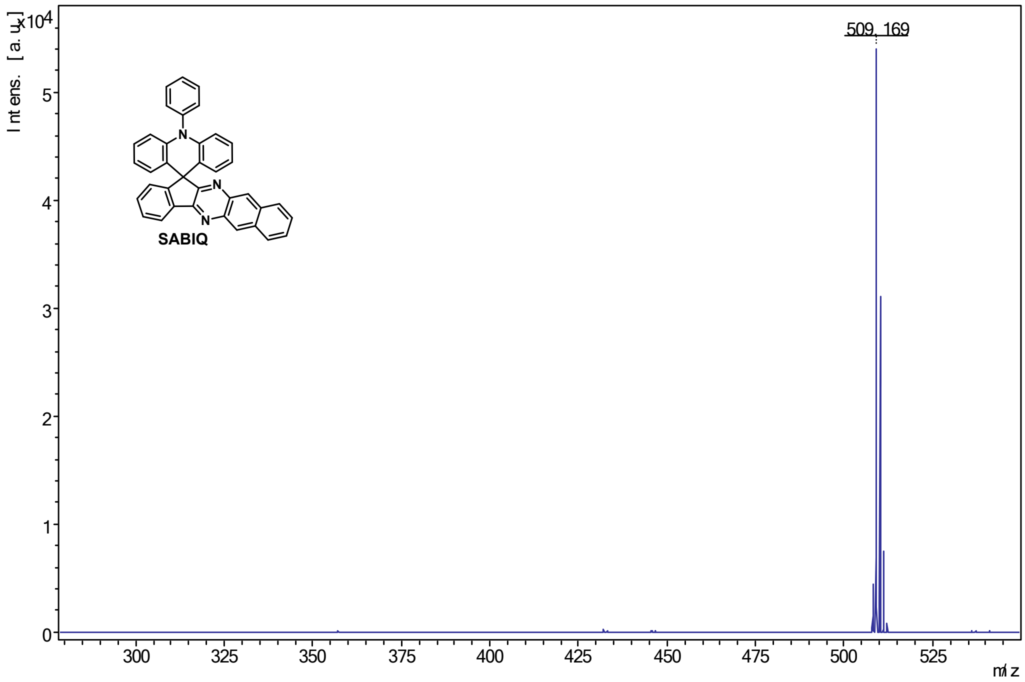

Figure S18. MALDI-TOF-MS spectrum of **SABIQ**.